Imaging the Hudson Bay basin using seismic interferometry

Agnieszka Pawlak and David W. Eaton

ABSTRACT

The Hudson Bay basin is the least studied of the four major Phanerozoic intracratonic basins in North America, which include the hydrocarbon-rich Williston, Illinois and Michigan basins. This study focuses on regional crustal structure based on ambient-noise tomography, a recently developed passive seismic method. Twenty-one months of continuous ambient-noise recordings were acquired from 31 broadband seismograph stations that encircle Hudson Bay. These stations are part of the Hudson Bay Lithospheric Experiment (HuBLE), an international project that is currently operating more than 40 broadband seismograph stations around the periphery of Hudson Bay. Following established processing procedures that include trace normalization and spectral whitening, cross-correlations were computed for all possible station pairs. The resulting waveforms are treated as Green's functions, from which group-velocity dispersion measurements can be made. Since Hudson Bay freezes during winter months, there is a pronounced asymmetry to the Green's functions indicative of seasonal variations in noise sources, and an apparent predominance of sources from the Atlantic seaboard. Preliminary results indicate shield-like conditions in most areas, with higher velocities beneath the oldest regions, the Archean Superior craton south and east of Hudson Bay. With this exception, the upper crust beneath the Hudson Bay basin is indistinguishable from surrounding shield areas. This characteristic differs from basins in southern California that have been studied using this method and may help to constrain models for formation of the Hudson Bay basin.

INTRODUCTION

Noise signals are traditionally cut out, removed and never seen again. For this study, however, we deliberately collected and used continuous recordings of ambient seismic noise data for a 21 month time period for seismograph stations situated around the periphery of Hudson Bay. Using a new technique known as seismic interferometry (Curtis et al. 2006), also referred to as ambient-noise tomography, this study focuses on crustal structure of the Hudson Bay basin. This method is based on cross-correlation of extensive noise time series, which provides an estimate of the Green function between the stations (Bensen et al. 2007). Using cross-correlations of noise recordings for all possible pairs of seismograph stations, a dense set of crossing paths is obtained to which tomographic-inversion methods can be applied.

Ambient-noise tomography was first applied to a dense network of seismograph stations in southern California (Shapiro et al. 2005). The results yielded group speed maps at short periods (7.5 – 15s) that revealed low-speed anomalies corresponding to major sedimentary basin and high-speed anomalies corresponding to the igneous cores of the main mountain ranges. Ambient-noise tomography has now been applied to several other regions and scales all over the world, such as a continental study of Europe (Yang et al. 2007), a study across all of California and the Pacific North-west (Moschetti et al.

2007) and smaller scale studies in New Zealand (Lin et al. 2007) and Tibet (Yao et al. 2006). This study represents the first application of this method to the Hudson Bay basin.

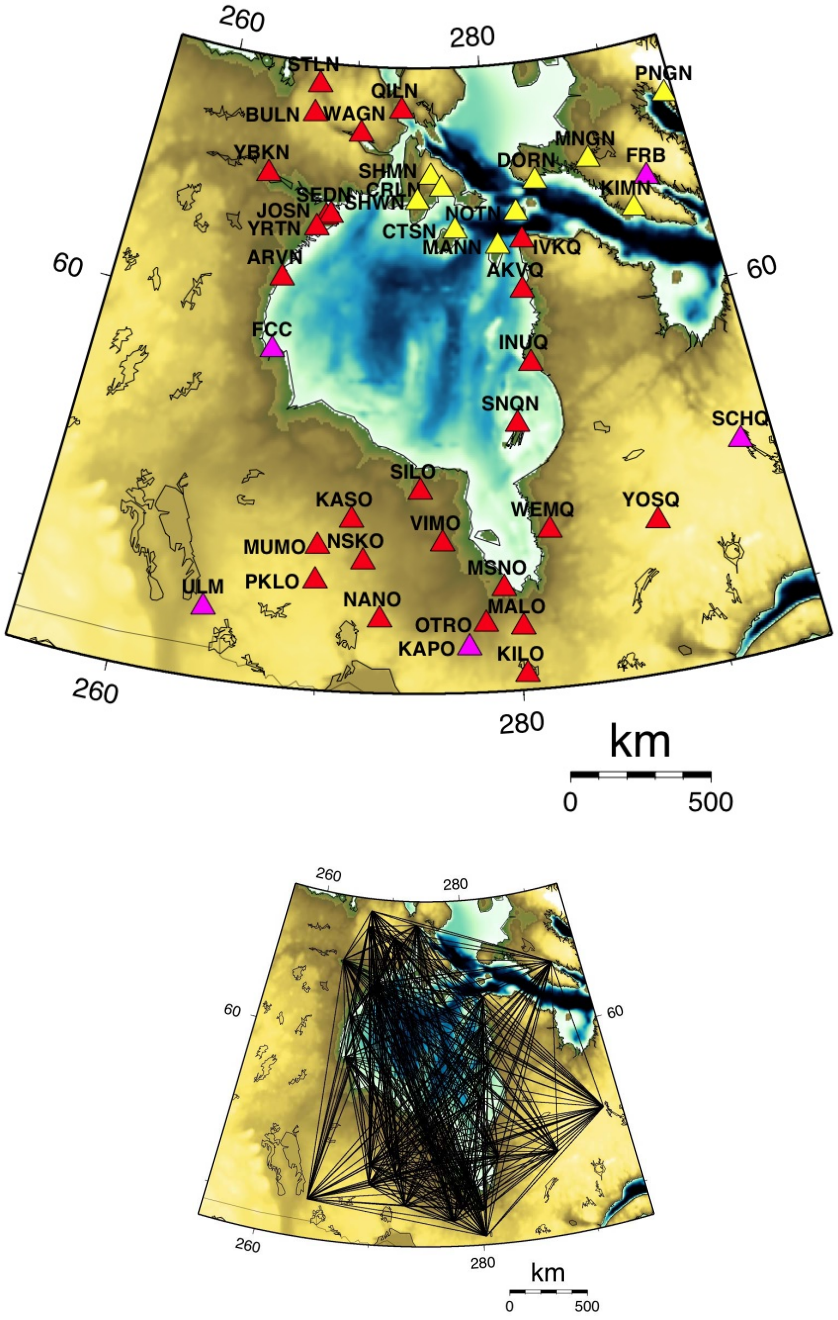

FIG. 1. Map of Hudson Bay. Red triangles represent temporary stations deployed as part of this project. Magenta triangles represent permanent stations of the Canadian National Seismograph Network (CNSN). Yellow triangles represent temporary stations funded by the British NERC agency. The inset shows the interstation paths for all possible station pairs; this does not include NERC stations, as data for these stations are not yet available.

Hudson Bay is a vast inland sea that penetrates deeply into north-central Canada, forming a conspicuous element of the North American coastline. The Bay conceals

several fundamental tectonic elements of North America including most of the Paleozoic Hudson Bay basin, an intracratonic basin with a similar stratigraphic record to the Williston, Illinois and Michigan basins. Hudson Bay was extensively studied in the 1960's and 1970's, including reconnaissance seismic programs and several deep stratigraphic test boreholes. Since that time no advances using geophysics have been made in this area. Our main goal is to constrain the deep crustal architecture of the Basin using a new approach.

In this paper we apply seismic interferometry to 31 broadband seismograph stations located around the perimeter of Hudson Bay (Figure 1), following the method outlined by Bensen et al. (2007). We describe the ambient-noise method in detail, and then show preliminary results for Hudson Bay for 21 months of noise data. The basin-scale approach described here is also applicable to smaller-scale investigations.

METHODS

We have analyzed data from 31 broadband seismic stations located around Hudson Bay. The data consists of three-component measurements of ground motion with a sampling rate of 40 samples per second. The dataset comprises 21 months, starting from September 2006 and ending May 2008. These stations are part of the Hudson Bay Lithospheric Experiment (HuBLE), an international project that is currently operating more than 40 broadband seismograph stations around the periphery of Hudson Bay. This data is all available online from the Geologic Survey of Canada through the automatic data request manager (autodrm) operated by Earthquakes Canada.

The data processing procedure we used follows the steps described by Bensen *et al*. (2007). First, the data were split and decimated by cutting the recordings into individual one-day records and resampling to 1 sample per second. Next, we removed the daily trend, mean and instrument response from the raw signals. Data were then normalized using a one-bit normalization to remove unwanted earthquake signals and instrument irregularities, which obstruct the broadband ambient-noise signal. This was accomplished by generating a data stream of 1's and -1's, retaining only the sign and disregarding the amplitude of the signal (Yang et al. 2006). Bensen et al. (2007) referred to this step as 'temporal normalization'. This step is followed by spectral normalization, which acts to broaden the frequency band of the noise data.

After the time series has been processed for each day, cross-correlations are done between all possible station pairs for all available daily records. Data selection is done later. The total number of interstation paths is $n(n-1)/2$, where n is the number of stations (Bensen et al., 2007). With 31 stations, we have a total of 465 station pairs (Figure 1, inset). Figure 2 shows a 21-month stack of cross-correlations plotted against interstation distance. There is a clear linear trend for both the positive and negative lags of the signal, showing that the noise data has some correlation and is not completely random. The positive lag is called the causal signal and the negative lag is the acausal signal (Bensen et al. 2007). These two signals represent the waves traveling in opposite directions (Lin et al. 2007).

In previous studies, the average of the two signals is taken to create a symmetric signal. If the ambient noise sources were distributed homogenously in azimuth, then both signals would, in principle, be identical (Bensen et al., 2007). Careful inspection of individual cross-correlation functions shows that we seem to have a source that is stronger in one direction than the other. We have therefore chosen to create a one-sided signal by simply taking the side (i.e., causal or acausal) with higher signal-to-noise ratio (SNR). Depending on the order of the station pair, we have found that this virtually always corresponds to waves that are traveling away from the Atlantic seaboard.

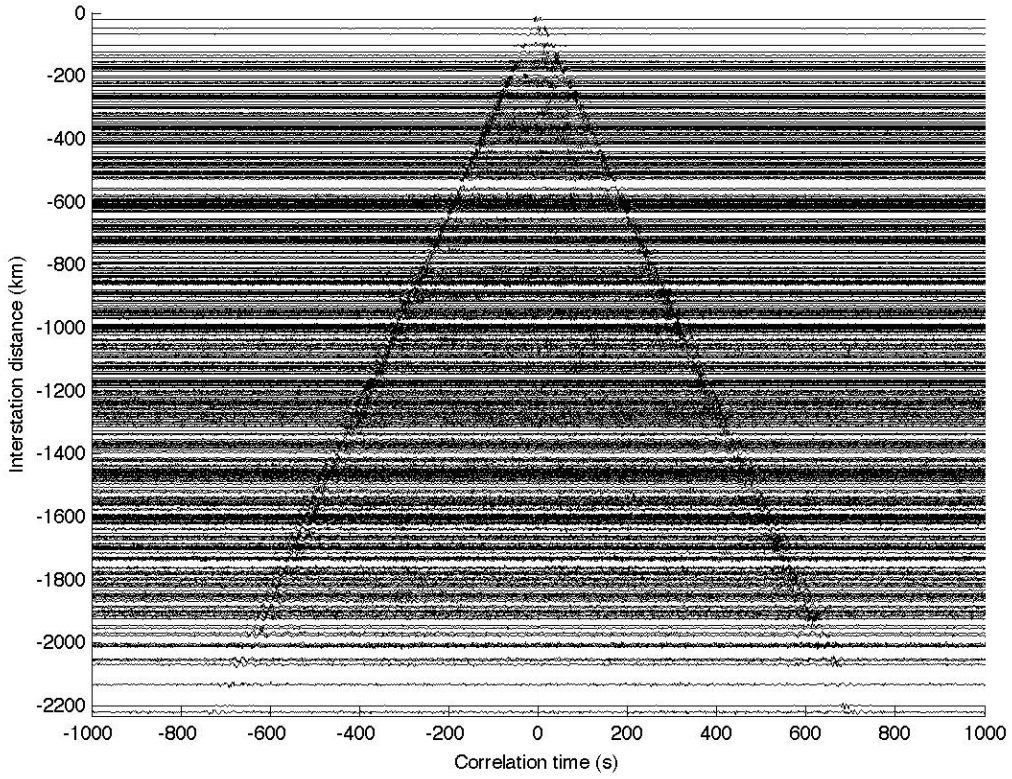

FIG. 2. Stacked cross-correlations plotted against interstation distance. All 465 traces are shown, with both positive and negative lags.

Cross correlating over long time periods is important to increase signal-to-noise ratio (SNR). For this application, SNR can be defined to as the ratio between the peak amplitude of the signal in a signal window and the root-mean-square of noise trailing the signal arrival window (Yang et al. 2006). Figure 3 shows the resulting cross-correlations for stations FCC and AKVQ for 1 month, 3 month, 12 month and 21 month time-series. These two stations are located 914 km apart and create an east/west cross-section across the Bay. The causal and acausal signals in Figure 3 emerge with increased time-series length. These signals can be identified as empirical Green's functions.

Group-velocity dispersion curves are measured from the estimated Green functions that emerge from the one-sided correlation stacks. Figure 4 demonstrates the dispersive character of the waves traveling from stations MALO to KASO, located south of Hudson

Bay. It is clear from this plot that the long-period waves arrive sooner than the short period waves. Using the estimated Green's functions, the group velocity measurements can be calculated using frequency-time analysis (Bensen et al. 2007). First, the one-sided correlation is filtered into small frequency bands. After calculation of the instantaneous amplitude (amplitude envelope), the dispersion ridge of the amplitude envelope is tracked as a function of period to obtain the group velocity curve. Dispersion results are shown in Figure 5 for stations MALO and KASO. The white line represents the group-velocity curve, which follows the peak amplitude as a function of period.

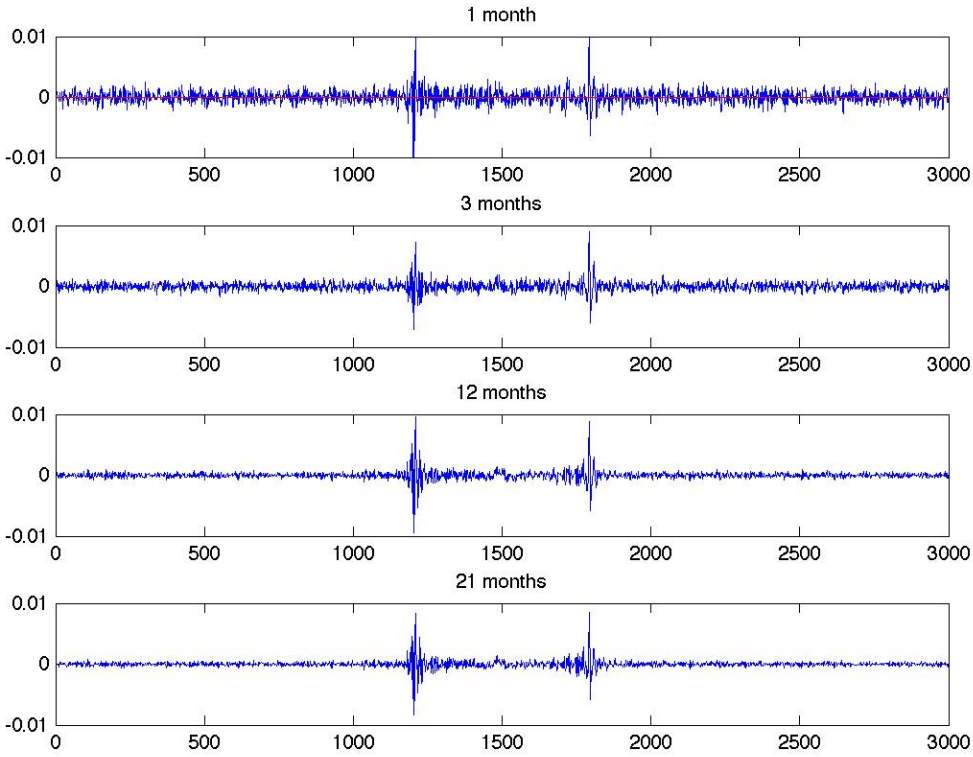

FIG. 3. Cross-correlations at the specified time-series length for stations AKVQ and FCC (Fig. 1). Note increasing SNR with increasing data length.

Previous studies have demonstrated that the Green's function is dominated by Rayleigh wave signals. Such waves are dispersive, and the dispersion curves can be used to infer structure of the crust and mantle beneath the path. Here, the Rayleigh-wave dispersion measurements were used to invert for group-velocity maps for 8 second, 12 second and 20 second periods, Figures 6-8. The inversion was done using the tomographic method described by Barmin *et al*. (2001).

DISCUSSION

Our tomographic maps contain prominent anomalies that can be related to major geological features. As a rule of thumb, the depth of maximum sensitivity of a group velocity map is the period expressed in kilometers (Lin et al. 2007). Hence, the 8-second

period map is most sensitive to the top 8 km of the crust, etc. This map (Figure 6) shows uniformly high velocity throughout the region, consistent with the shield-like nature of the crust. There are, however, two discernible anomalies, a high-velocity anomaly south of Hudson Bay and a low-velocity anomaly in the northeast corner of the bay. The high-velocity anomaly is most likely associated with Archean crust in the Superior Province. Darbyshire et al. (2007) found there to be a high-velocity mantle lid in this area of the Canadian Shield. The low-velocity anomaly occurs near the Cape Smith belt, where it extends into Hudson Bay. This is a major crustal shear zone, and the deformation associated with this structure may lower the velocity.

It is somewhat surprising that the Hudson Bay basin does not appear as an anomaly in the 8-s period group velocity map. We do not believe that this is caused by lack of data coverage, as there are sufficient crossing paths over this region. It is more likely that the basin is too thin to be resolved with this approach, having a maximum thickness of about 2 km (Sanford 1987). As noted above, the range of velocities seen on this map is quite small (~3.18 km/s – 3.20 km/s), as is expected for the Canadian Shield. The upper crust below Hudson Bay therefore appears to be indistinguishable from most of the surrounding shield areas. This observation may allow us to eliminate some models for basin formation.

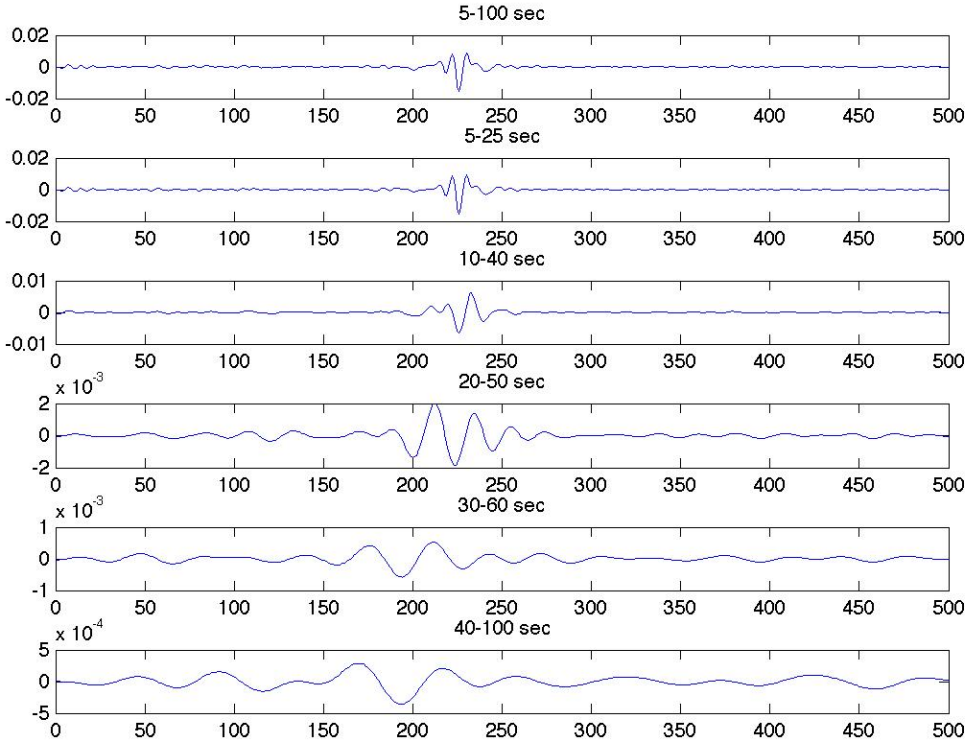

FIG. 4. Example of a broadband cross-correlation for stations MALO and KASO (Fig. 1). The broadband signal is shown at the top and progressively longer period bands are shown lower in the figure. Note the dispersive character of the signals, with longer periods (lower frequencies) arriving ahead of shorter periods.

The 12-second map (Figure 7) shows anomalies that occur in the middle crust, approximately in the top 12 km. The range of velocities is slightly greater for this period, ranging from 3.16 km/s to 3.23 km/s. Here we see a zone of low velocity near the Chesterfield inlet, which is in the northwest corner of Hudson Bay. Recent mid-crust earthquakes have occurred in this area, suggesting this might be a zone of weakness. Another low-velocity zone appears near the middle of Hudson Bay, east of the basin centre. The high velocity anomalies are still located in the Superior Province of Northern Ontario. This region of higher velocity has expanded to include the eastern shore of Hudson Bay as well.

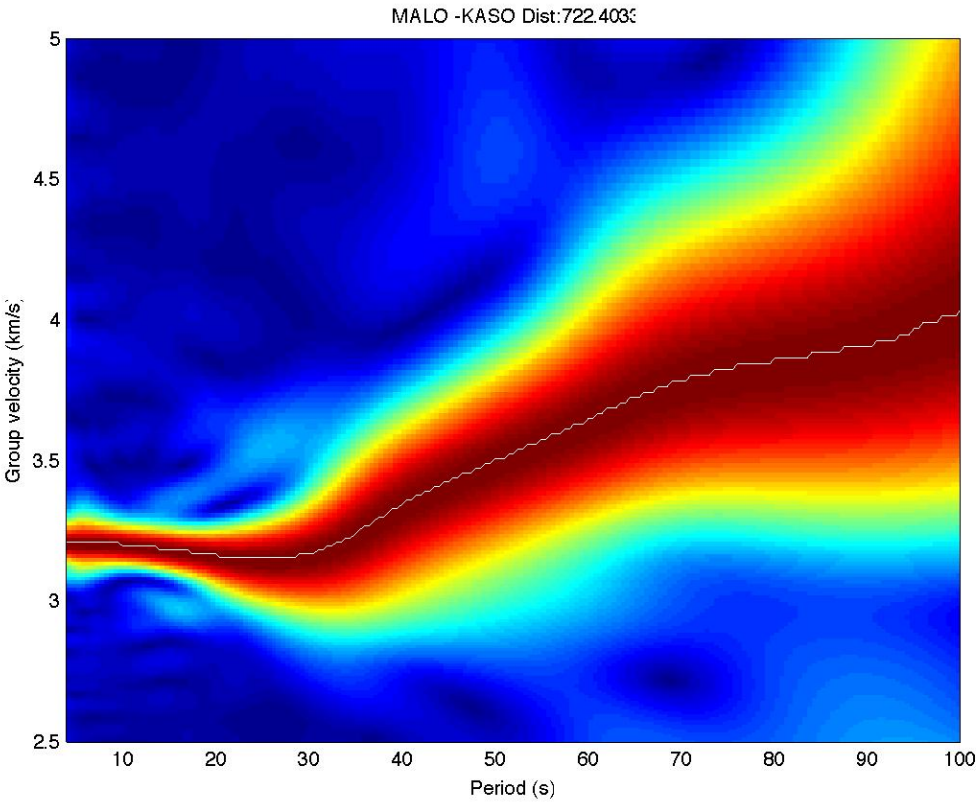

FIG. 5. Dispersion analysis results for stations MALO and KASO (Fig. 1) using the frequency-time analysis method described in the text. The white line shows the group-velocity curve.

There appears to be a linear artifact on the 12s period map near the south part of Nastapoka arc, which is located in the southeast corner of the bay. This artifact is probably due to the fact that we have more paths crossing the bay in the northwest-southeast direction than in the southwest-northeast direction. By adding data from the NERC stations, located on the islands north of Hudson Bay, as well as stations in northern Manitoba, we can increase the path coverage and mitigate the effect of these artifacts.

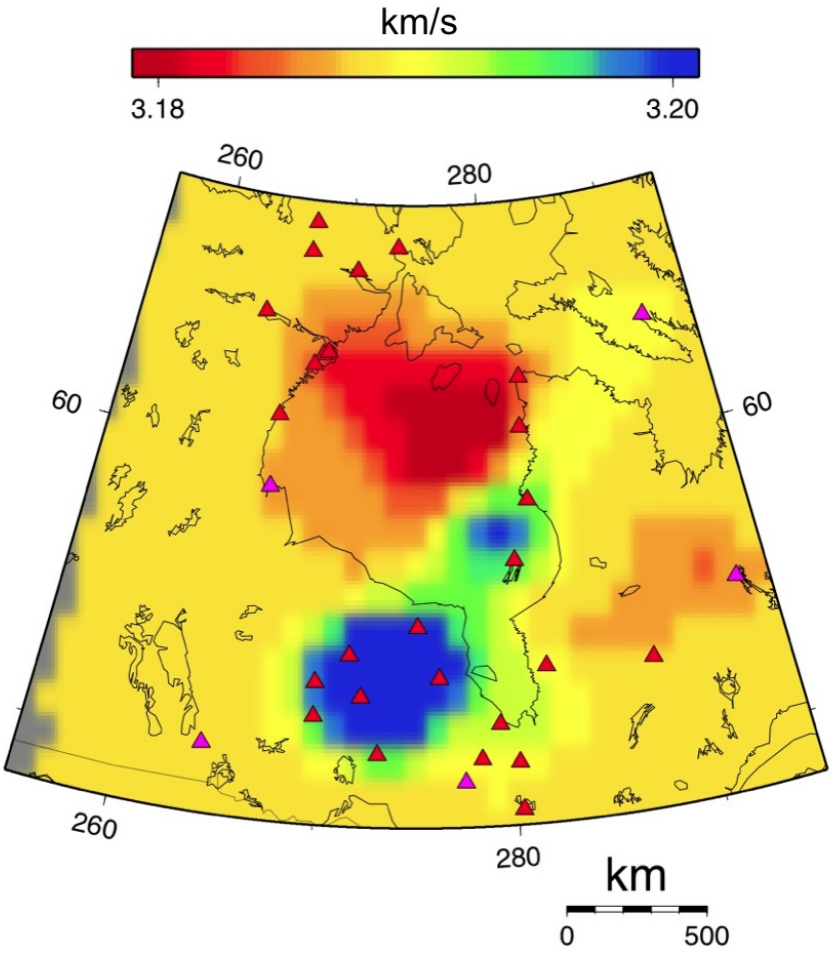

FIG. 6. Tomographic inversion results for 8-second period.

The 20-second map (Figure 8) is predominately sensitive to anomalies in the lower crust, around 20 km deep. The low-velocity anomaly from the 12-second map near the Chesterfield inlet persists. The high-velocity zone beneath the Superior Province also persists in this image. The velocity range is greater here (3.05 km/s to 3.20 km/s) than on the previous two maps, but these are still small variations compared to variations observed in tectonically active regions such as California. The inferred Rayleigh-wave group velocities are generally consistent with a shield setting (> 3 km).

FUTURE WORK

There is still a lot of work that can be done for this study. Looking at shorter period inversions to try to resolve the Hudson Bay basin and adding more stations to increase the path coverage and eliminate artifacts from current results will be the next step. Further analysis of the ambient-noise data will focus on localization of ambient-noise sources; results to date suggest strong seasonal variations, probably due to seasonal cycles of Arctic sea ice. Testing resolution and sensitivity kernels still need to be done as well. In addition, we would like to combine our ambient-noise results with longer-period

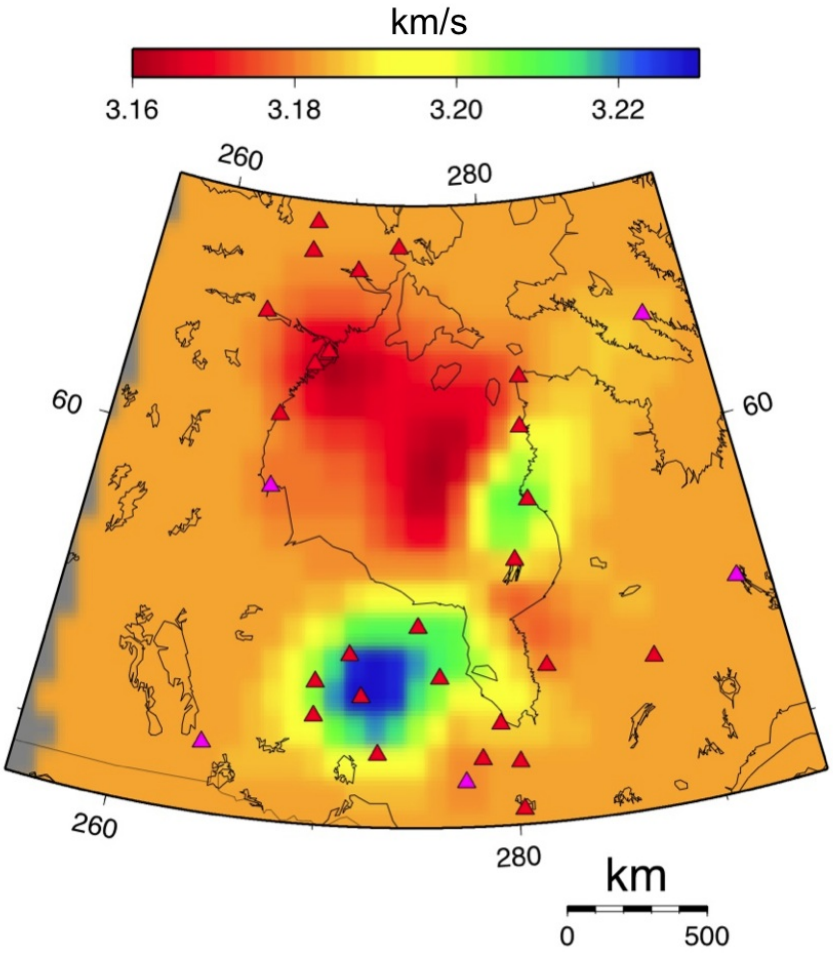

FIG. 7. Tomographic map for 12-second period.

results based on Rayleigh waves from earthquakes, a study being conducted by Fiona Darbyshire at UQAM

CONCLUSIONS

In this study, we use 21 months of ambient-noise data recorded at 31 broadband seismic stations that encircle Hudson Bay. Data were processed in daily segments then cross-correlations were performed for all possible station pairs. The cross-correlation functions were then stacked to increase the SNR, thereby revealing inter-station Green's function dominated by Rayleigh-wave signals. Coherent cross-correlation signals are observed up to distances of 2200 km. One-sided correlation signals were computed, by selecting the causal or acausal correlation signal based on SNR. These inferred Green's functions were then used to calculate group velocity dispersion curves.

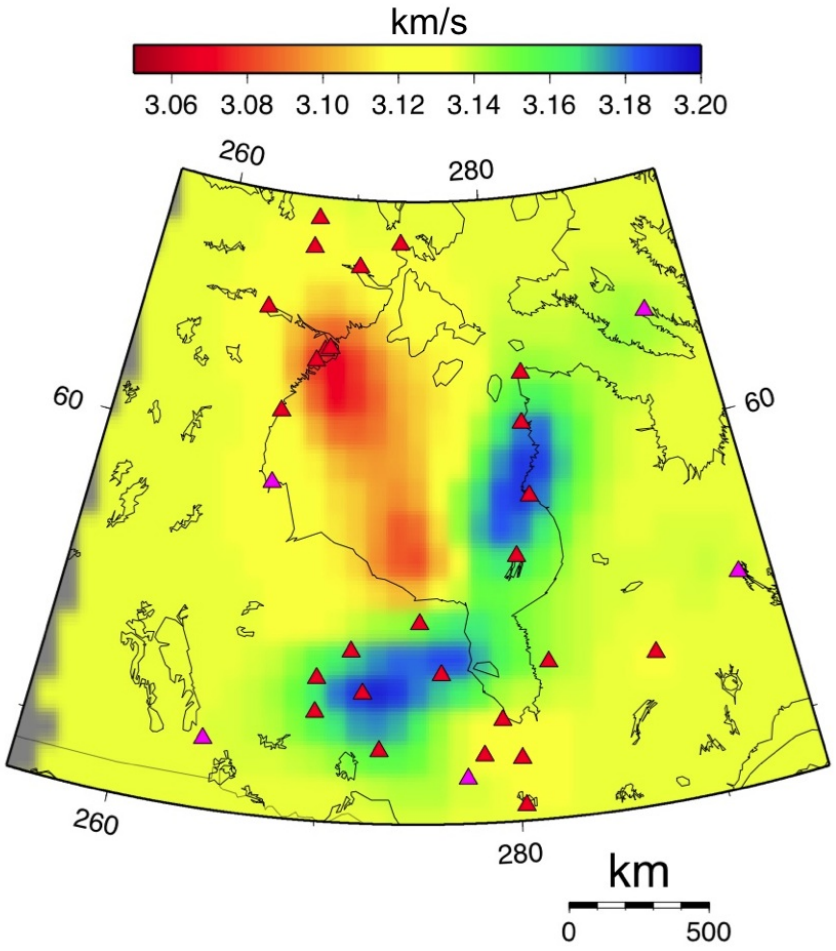

FIG. 8. Tomographic map for 20s period.

Group velocity maps for 8 s, 12 s and 20 s periods were obtained using ambient-noise tomography. The tomographic images can be related to regional geologic elements. All three maps contain a high-velocity zone in southern part of Hudson Bay, which is most likely associated with Archean crust in the Superior Province. Two low-velocity anomalies appear, one near the Cape Smith belt, shown on the 8s period map, and another one near the Chesterfield inlet, shown in the 12s and 20s period maps.

This study demonstrates that surface wave-tomography based on seismic ambient-noise data can be achieved with reliable result. This study serves as a foundation for future research into the crustal structure and origin of the Hudson Bay intractronic basin.

AKNOWLEDGEMENTS

We are grateful to Dr. Honn Kao, from the Pacific Geoscience Center in Sydney, B.C., for providing us with initial data and Unix processing scripts. This study was supported by NSERC through a discovery grant to DWE.

REFERENCES

Barmin, M.P., M.H. Ritzwoller, and A.L. Levshin, (2001), A fast and reliable method for surface wave tomography: Pure Appl. Geophys., **158**, 1351 – 1375.

Bensen G. D., Ritzwoller M. H., Barmin M. P., Levshin A. L., Lin F., Moschetti M. P., Shapiro N. M., and Yang Y., 2007, Processing seismic ambient noise data to obtain reliable broad-band surface wave dispersion measurements: Geophys. J. Int. ,**169**, 1239-1260.

Curtis, A., P. Gerstoft, H. Sato, R. Snieder, and K. Wapenaar, 2006, Seismic interferometry – turning noise into signal: The Leading Edge, 1082-1092.

Darbyshire, F.A., D.W. Eaton, A.W. Frederiksen and L. Ertolahti, 2007, New insights into the lithosphere beneath the Superior Province from Rayleigh wave dispersion and receiver function analysis: Geophys. J. Int., **169**, 1043-1068.

Lin, F., Ritzwoller M.H., Townend J., Savage M., and Bannister S., 2007, Ambient noise Rayleigh wave tomography of New Zealand, Geophys. J. Int., **18**.

Moschetti, M.P., M.H. Ritzwoller, and N.M. Shapiro, 2007. Surface wave tomography of the western United States from ambient seismic noise: Rayleigh wave group velocity maps,: Geochem., Geophys., Geosys., **8**.

Sanford, B.V., 1987, Paleozoic geology of the Hudson Platform: Canadian Society of Petroleum Geologists Memoir, **12**, 507-518.

Shapiro, N.M., M. Campillo, L. Stehly, and M.H. Ritzwoller, 2005, High resolution surface wave tomography from ambient seismic noise: Science, **307**, 1615-1618.

Yang, Y., M.H. Ritzwoller, A.L. Levshin, and N.M. Shapiro, 2007, Ambient noise Rayleigh wave tomography across Europe: Geophys. J. Int., **168**, 259

Yao, H., R.D. van der Hilst, and M.V. de Hoop, 2006, Surface-wave tomography in SE Tibet from ambient seismic noise and two-station analysis: I.- Phase velocity maps: Geophys. J. Int., **166**, 732-744.